ARCTIC OCEAN GEOID, ICE THICKNESS AND MEAN SEA LEVEL – THE ARCGICE PROJECT

R. Forsberg[(1)], H. Skourup[(1)], O. Andersen[(1)], P. Knudsen[(1)], S. W. Laxon[(2)], A. Ridout[(2)], A. Braun[(3)], J. Johannessen[(4)], C. C. Tscherning[(5)], D. Arabelos[(6)]

[(1)] Dept, Danish National Space Center, Juliane Maries Vej 30, DK–2100 Copenhagen Ø, Denmark
[(2)] Center for Polar Observation and Modelling, University College London, UK
[(3)] Department of Geomatics Engineering, University of Calgary, Alberta, Canada
[(4)] Nansen Environmental and Remote Sensing Center, Bergen, Norway
[(5)] Niels Bohr Institute, University of Copenhagen, Denmark
[(6)] Department of Geodesy and Surveying, Thessaloniki University, Greece

ABSTRACT

Satellite altimetry from ERS, Envisat and ICESat may be used together with updated geoid models based on surface, airborne and satellite gravity field data to derive estimates of Arctic Ocean mean dynamic topography (MDT). In the paper we outline the computation of a new Arctic geoid from terrestrial gravity data and GRACE, and study characteristics of the geoid errors based on least-squares collocation. Based on ICESat lowest-level filtered laser altimetry and retracked ERS radar altimetry we construct an Arctic Ocean mean sea surface (MSS), which combined with the geoid model gives an estimate of the MDT. We compare results to oceanographic models, showing that an overall absolute consistency is possible at the dm-level. Arctic Ocean sea ice freeboard heights (and thus thickness) are an integral part of these investigations, and ICESat-derived freeboard heights show a good correlation to multi-year ice distribution as determined from Quikscat. The sea ice presence, which may bias altimetry sea level measurements, as well as the inhomogenous distribution of gravity data and tidal model errors, are limiting factors in the MDT determination.

1. INTRODUCTION

With the launch of the dedicated polar altimetry satellites: NASA's ICESat, launched 2003 [1], and ESA's Cryosat-2 (2009), there is the possibility to do monitoring of sea-ice thickness, as well as mean dynamic ocean topography (MDT) over most of the Arctic Ocean. Because of the sea ice cover, it is a special challenge to measure the sea surface ellipsoidal heights (SSH) with sufficient accuracy. Models of the geoid heights N might be useful in the SSH determination, as the geoid is the dominant signal in the SSH. This is especially true for studies using ICESat laser data, where preliminary results of ICESat-derived Arctic Ocean sea-ice thickness (up to 86°N) have recently been published [2].

Methods for radar satellite altimetry measurement of sea-ice thickness have originally been developed for ERS pulse-limited radar altimetry [3], which due to orbit limitations only cover parts of the Arctic (south of 81°N). In the ERS investigations, the radar return pulse shape is utilized to discriminate between "specular" reflections from open water or leads in the ice pack, and reflections from the top of ice floes. This allows a direct measurement of the sea-ice freeboard height, which under assumptions of isostatic balance of the ice floe in the water, and assumptions on snow, ice and water density, may be converted to sea ice thickness, cf. Figure 1, as well as the direct measurement of ocean surface height as a function of space and time.

The investigations in this paper are a brief summary of studies on the geoid, MSS and MDT in the Arctic Ocean, and the associated errors. The studies are part of an ongoing ESA study "ArcGICE", aimed a.o. at providing a practical algoritm for the estimation of sea surface heights and its associated error covariances, to be used, e.g., as reference for future Cryosat measurements of the sea ice freeboard. Additional topics studied include tidal errors and optimal joint collocation solutions for MDT and geoid, not included here due to space limitations.

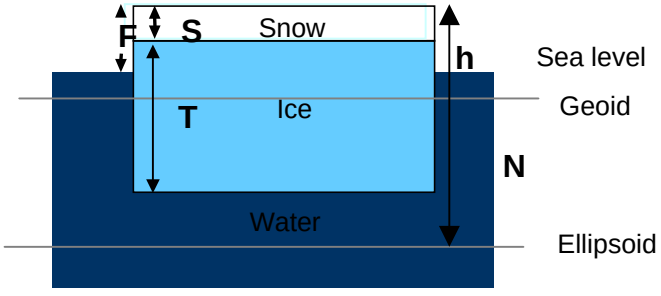

Fig 1. Sea-ice freeboard F, thickness T and its relation to geoid N, MDT (sea level minus geoid) and mean sea level.

It should be pointed out that there are two types of freeboard heights: the freeboard including snow (F, cf. Fig. 1), and the freeboard height of the ice only (F-S). The latter is the freeboard height used for radar altimetry, since it is generally believed that the radar reflects off the snow/ice interface (except for the summer melting season). For airborne and satellite laser altimetry, the snow freeboard is measured.

For satellite altimetry the basic measurement h is thus the ellipsoidal height of the snow surface (laser) or the ice (radar), and the basic equation for freeboard determination is thus

$$F = h - N - MDT + e \qquad (1)$$

With good orbit and pointing data, the altimetry measurement of the snow/ice surface is ideally accurate to few cm. Due to the developments in geoid determination, notably the launch of the GRACE satellite [4], the accuracy of geoid models has become very high as well, at the absolute error level of a few cm at wavelength scales longer than a few hundred km.

If the deviation between the ocean surface and the geoid, i.e. the oceanographic mean dynamic topography (MDT) and the tides, can be modeled with sufficient accuracy, it should therefore in principle be possible to measure the sea-ice freeboard heights directly from space without special identification of measurements originating from leads and thin ice. This would especially be an advantage for laser altimetry, where there is at present no simple method to discriminate between laser returns from thin or thick ice [5]. The comparison of oceanographic MDT models to estimates of MDT from combinations of SSH and geoid models are therefore a central part of the ArcGICE project.

2. GEOID OF THE ARCTIC OCEAN

Due to recent airborne and submarine survey activities, as well as release of formally cold-war era classified gravity data sources, the knowledge of the geoid in the Arctic Ocean is quite good. The Arctic Gravity Project [6] has thus compiled a 5' gravity anomaly data grid for the Arctic region north of 64°N, based on all available surface, submarine and airborne gravity data, supplemented in some regions (mainly north of Siberia) with gravity derived from ERS satellite altimetry [7]. For details of the project and data coverage see the ArcGP web site (http://earth-info.nga.mil/GandG/agp), where a recent grid update was posted February 2006. Figure 2 shows the new free-air gravity anomaly grid of the region, illustrating the quite rough gravity field.

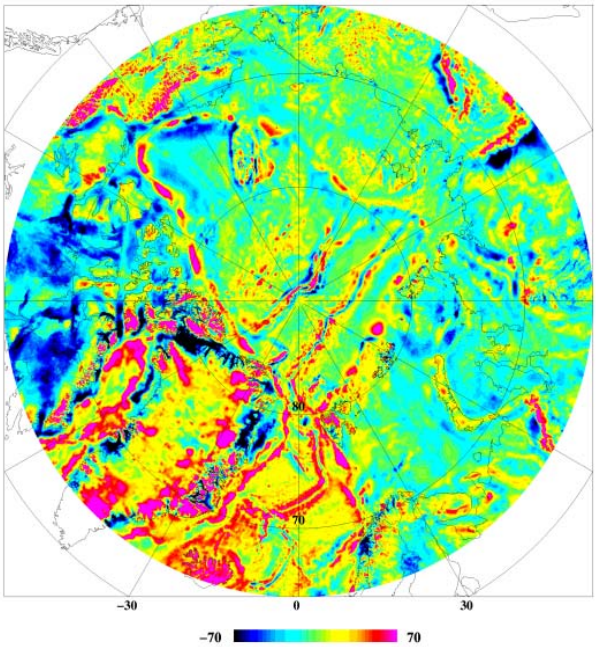

Fig. 2. Arctic gravity anomalies. Unit mGal (10^{-5} m/s^2)

We generated a new dense (5' resolution) geoid model of the Arctic region using the GRACE GGM02S spherical harmonic model as a reference model. In the used "remove-restore" method, the residual ArcGP gravity anomalies were converted into geoid residuals by spherical FFT methods [8]. The FFT method implement Stokes' formula

$$N = \frac{R}{4\pi\gamma}\iint_{\sigma}\Delta g S'(\psi)\,d\sigma \qquad (2)$$

where Δg is the gravity anomaly, R Earth radius, γ normal gravity, and ψ the spherical distance, with the integral in principle covering the whole earth. We used a modified Stokes' function given by

$$S'(\psi) = \sum_{l=n}^{\infty}\frac{2l+1}{l-1}w_l P_l(\cos\psi) \qquad (3)$$

This allows only the short-wavelength gravity anomalies to affect the computed geoid at spectral bands higher than spherical harmonic n. The spectral weights w_l were assigned to make a linear transition in the spherical harmonic band n = 80 to n = 90, implying spherical harmonic data are used fully below harmonic degree 80, and terrestrial data fully above degree 90. To reduce edge effects, we used a high-degree composite GRACE/EGM spherical harmonic reference model complete to degree 360, formed by merging GGM02S linearly with EGM96 in the same harmonic band. An example of a computed Arctic Ocean geoid model is shown in Figure 3.

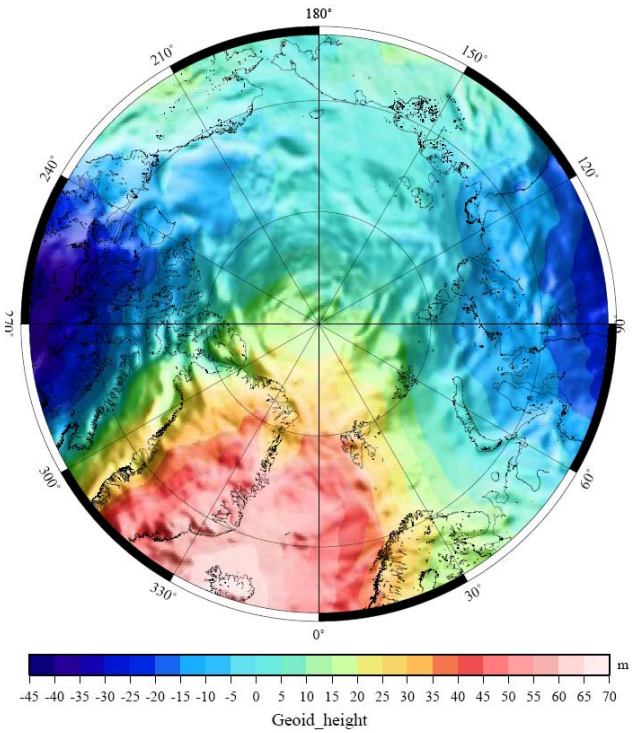

Fig. 3. Geoid of the Arctic region from terrestrial gravimetry and satellite data by collocation. Unit m.

3. ERROR COVARIANCES OF THE GEOID

To estimate the quality of the computed geoid, a special geoid computation and error study was made by least squares collocation. A subset of the point gravimetric data underlying the Arctic Gravity Project was used for these error studies.

In the least squares collocation method [9] the gravity field observations y, e.g. gravity, is expressed as linear functionals on the geopotential T

$$y_i = L_i(T) + e_i + A_i^T \cdot X \qquad (4)$$

and the optimal solutions are obtained by solving a system of linear equations of similar dimension as the number of observations, giving estimates of T and systematic parameters X by

$$\tilde{T}(P) = \{C_{Pi}\}^T \overline{C}^{-1}(y - A^T X) \qquad (5)$$

$$\tilde{X} = (A^T \overline{C}^{-1} A + W)^{-1}(A^T \overline{C}^{-1} y) \qquad (6)$$

Using a subset of 56800 point gravity values, providing a near-uniform sampling of the Arctic, the geoid of Fig. 3 was obtained. From the computations, also formal error estimates and error covariances are obtained, as well as biases on some of the major gravimetric surveys. In this way several surveys entering ArcGP were found to have biases ranging from 2 to 6 mGal.

Fig 4 shows the estimated accuracy of the geoid, showing that a 10 cm geoid model is apparently obtainable over most of the region. Because the FFT geoid computation is able to use more gravity data than collocation, the error estimates might actually be pessimistic. Fig 5 shows an example of the estimated suite of error covariances along a specific meridian. This illustrates that the geoid errors have a typical correlation length around 30-50 km.

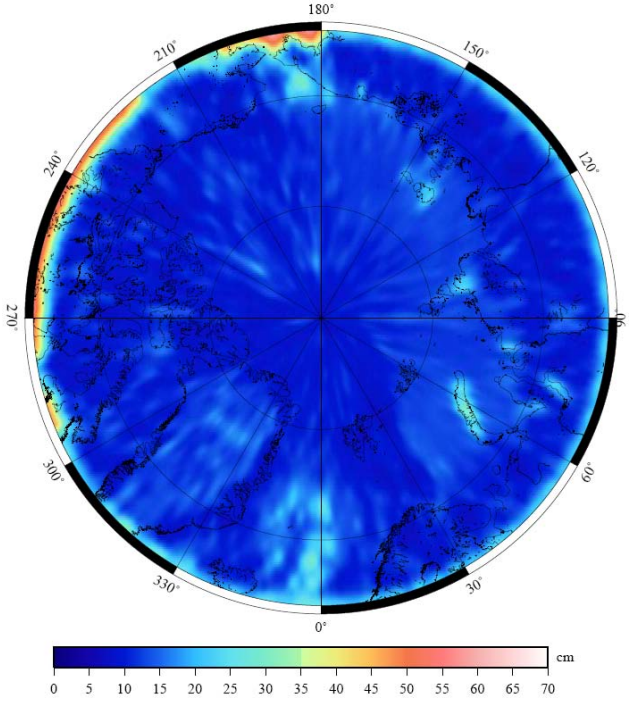

Fig. 4. Geoid error estimates from collocation. Unit cm.

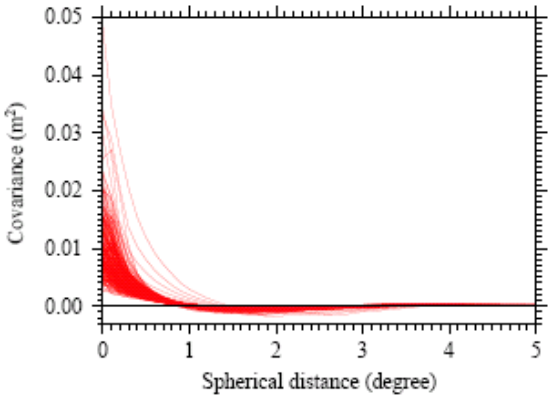

Fig. 5. Geoid error covariance functions along the 15°E meridian, for latitude ranging from 64° to 90° N.

4. ICESAT FREEBOARD HEIGHTS AND MDT

We have analyzed two periods of ICESat data, Feb. 20 – March 29, 2003 (laser 1, release 18) and Sep. 25 – Nov. 18, 2003 (laser 2a, release 21). Figure 6 shows the difference between the ICESat SSH and the geoid for the laser 1 period. It is seen that the differences shows both orbit-related and more localized errors, and that a freeboard signal is not very apparent. Some of the errors are due to track biases (e.g., due to errors in orbits, pointing, and inverted barometer effects), and others due to geoid errors.

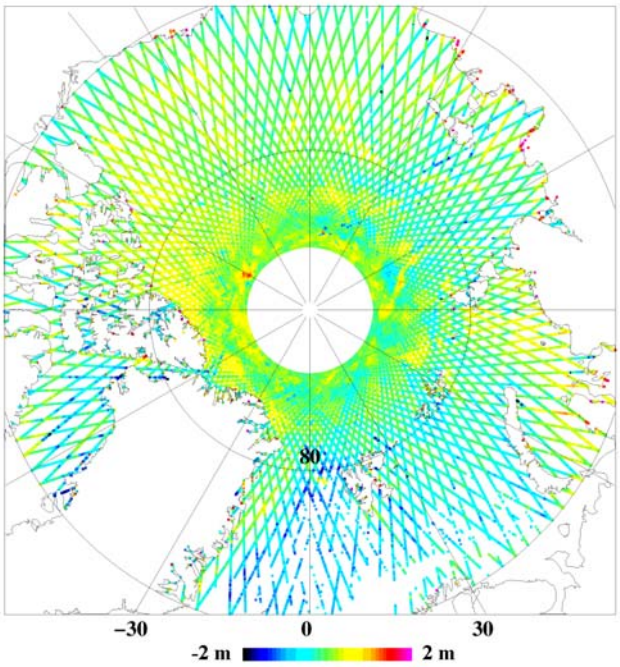

Fig. 6. Difference ICESat SSH (laser 1) minus the geoid.

To estimate freeboard heights, a lowest-level filtering must be done on the geoid-reduced ICESat track data. We use here a new along-track filtering scheme where the 3 lowest values for a 20 km segment is used to define a lowest value correction compared to the "spatial" algoritm used in [2]. The resulting freeboard heights for the laser 1 period is shown in Figure 7. The regions of thicker ice show a good correlation to regions of multi-year ice coverage, as determined by Quikscat, cf. [2]. Similar analysis for the laser 2a period shows a clear seasonal signal due to the sea ice melt over the summer.

Fig. 8 shows the corresponding MDT (= h – F – N) estimated for the Feb.-March laser-1 period. To limit the orbit-related errors, a cross-over adjustment have been applied to these data, estimating a bias for each orbit.

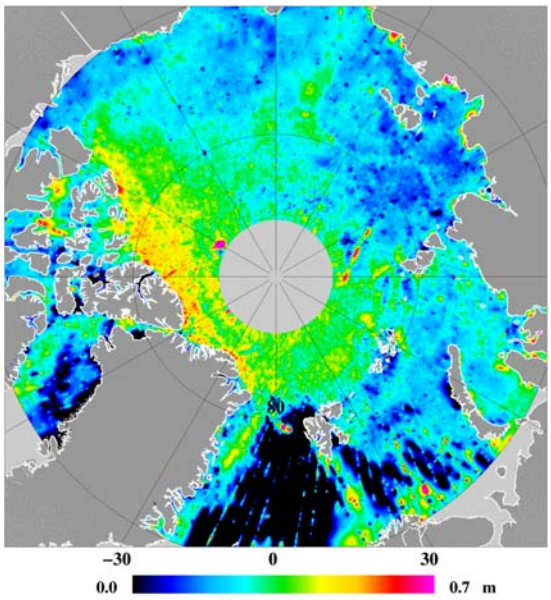

Fig. 7. ICESat sea ice freeboard heights, March 2003.

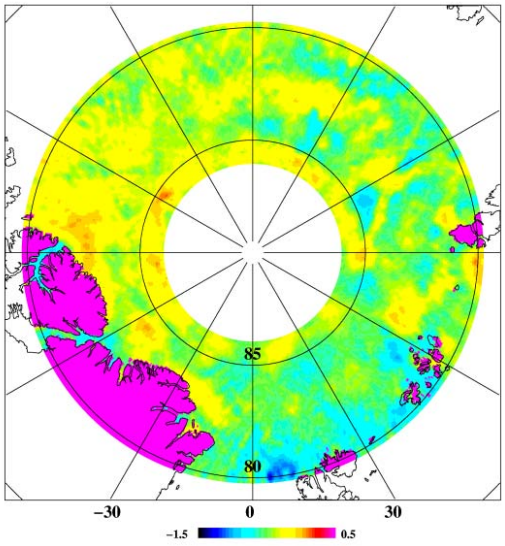

Fig. 8. Apparent ICESat MDT for March 2003. Unit m.

5. ARCTIC OCEAN MDT FROM ERS AND ICESAT

The ICESat MDT, as shown in the example of Fig. 8, only covers a limited time span, and is probably still offset by major biases, such as biases from the lowest-level filtering algorithm. To make an Arctic-Ocean wide MDT, covering a larger area and a longer time span, we have therefore merged MDT data sets from ERS and ICESat. The ERS-2 mean SSH data set span the period 1995-2003, and is an integral part of the UCL processing of ERS-2 data for sea-ice freeboard estimation [3].

The computed MSS have been reduced for the ArcGP geoid, and to merge the data sets, the following "draping" procedure has been applied: The difference in MDT between ERS and ICESat across the band 80-81.5°N

$$\varepsilon = MDT_{ERS} - MDT_{ICESat} \quad (7)$$

has been interpolated outside the overlap zone with least-squares collocation (optimal estimation), and the predicted corrections ε have subsequently been added to the ICESat data, effectively forcing these data to match the much longer ERS-time span. A constant offset has at the same time been estimated, taking into account the different reference systems used (Topex ellipsoid for ICESat and WGS84 for ERS). Table 1 shows the statistics of the comparisons in the MDT across the comparison band, and Figure 9 show the compiled Arctic-wide MDT, where a similar collocation draping have been used to fill in across the polar gap data void north of 86°N.

Table 1. Statistics of difference between SSH and geoid

Unit: m	Mean	Std.dev.
ICESat – geoid (in the overlap 80-81.5°N)	-0.52	0.19
ERS – new geoid (in overlap band)	-1.19	0.39
ERS – ICESat (in overlap band)	-0.71	0.28
Composite MDT – geoid in WGS84 (in entire Arctic Ocean)	0.26	0.29

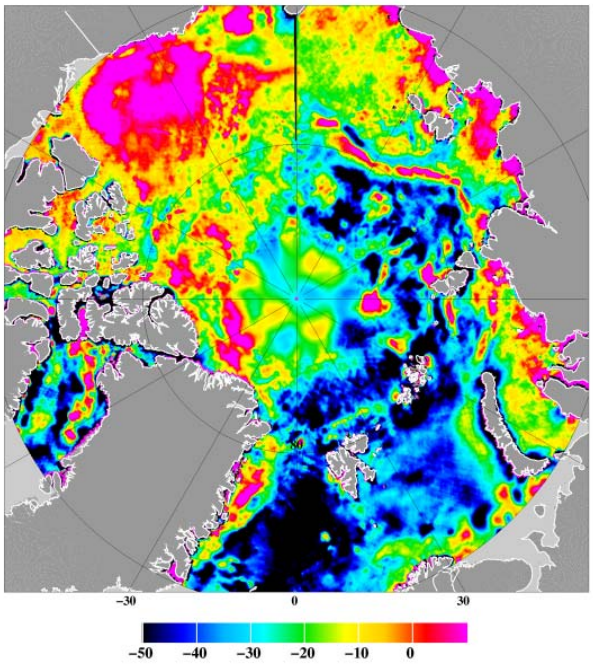

Fig 9. Composite MDT made by draping of ICESat to ERS, and fill-in with draped geoid north of 86°. Unit: cm.

6. OCEANOGRAPHIC MODEL COMPARISON

The satellite-derived MDT of Fig. 9 may be compared to independent oceanographic models of MDT. Figure 10 shows an example of the MDT derived from the 1/4°-resolution MICOM model, as implemented at NERSC. Fig. 11 shows for comparison the MDT from the higher-resolution PIPS model for the ICESat periods (courtesy W. Maslowsky, Naval Postgraduate School).

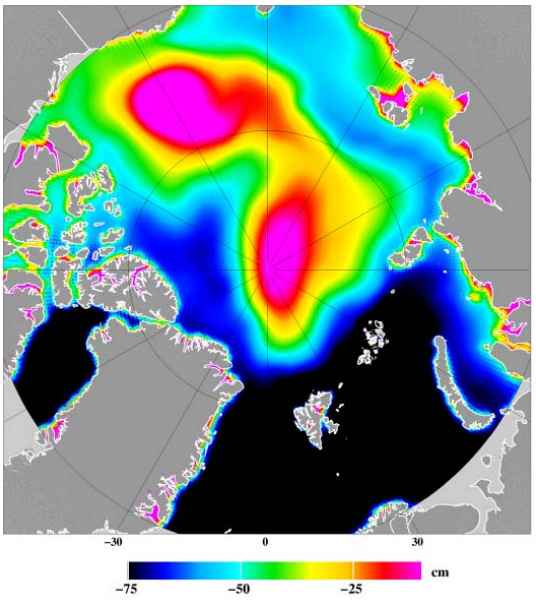

Fig. 10. Average MDT from MICOM 1995-2003. Unit cm.

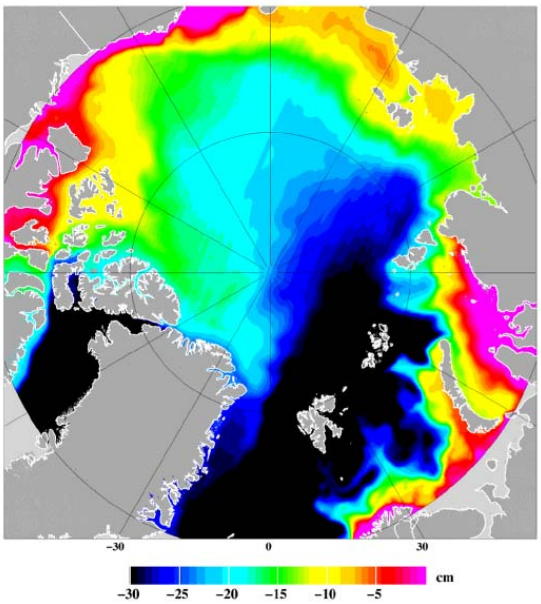

Fig. 11. MDT from the PIPS model (2003 average).

Major differences in models are generally seen, especially with the major positive feature in the Canadian Basin (the Beaufort gyre) being quite different in time and space in the models. The MDT features are relatively stable in time, and related to the main ocean circulation. Fig. 12 shows an example of the seasonal variability of the MDT from the MICOM model.

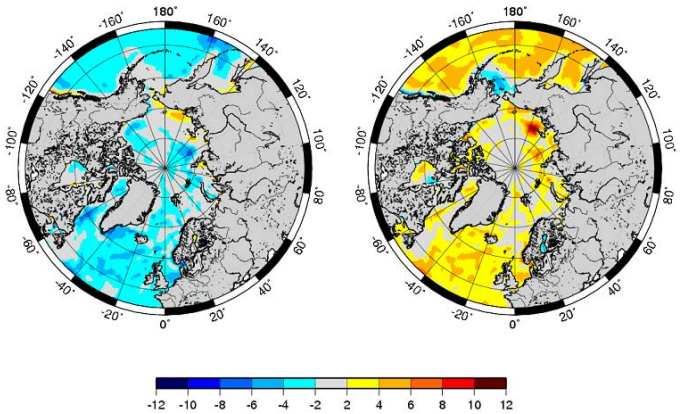

Fig. 12. The seasonal variability in MDT: mean anomaly in MDT for March (left) and September (right), compared to the mean field for the 1948-2005 MICOM hindcast simulation. Colour scale range from –12 to 12 cm.

Unfortunately the MDT from remote sensing (SSH-N) do not clearly discriminate between models, a.o. due to lack of SSH data north of 86°N, and the mixed epochs of the combined ICESAT-ERS mean SSH model. However, an overall reasonable quantitative agreement is found, with e.g. the low in the Norwegian-Greenland Sea seen to propagate northwards into Siberian Arctic Ocean consistently in both Fig. 9 and Fig. 10-11. It is therefore clear that the freeboard/MDT estimation is consistent with the independent MDT data, and the potential of the (mostly) space-based MDT methods based on satellite altimetry and GRACE is therefore highlighted.

7. CONCLUSIONS

We have outlined the estimation of the Arctic Ocean MDT and sea-ice freeboard heights from ICESat laser altimetry, and ERS-2 radar altimetry, by using a new geoid model of the Arctic Ocean, based on GRACE data and local gravity observations. The estimated sea ice freeboard heights show a pattern consistent with the expected distributions of sea-ice thickness, with the thickest ice located north of Greenland and Ellesmere Island. The MDT estimates shows a good quantitative agreement with oceanographic MDT models, thus illustrating the potential application of satellite altimetry missions, especially the upcoming Cryosat-2, to estimate not only sea-ice thickness and its trends, but also the ocean mean dynamic topography and its temporal changes. The errors of the geoid and MDT have been illustrated through formal estimates of geoid error covariances, as well as variability of oceanographic models. Considering additional errors, e.g. from ocean tide models, it is clear that additional satellite and terrestrial data are needed before a sufficiently accurate SSH model can be established for direct sea ice freeboard mapping from satellite altimetry. Optimal collocation combination methods will be a useful tool in this respect, part of the ongoing ArcGICE studies.

ACKNOWLEDGEMENTS

We thank W. Maslowski, Naval Postgradute School, USA, for providing PIPS monthly oceanographic results, and R. Bingham for help in providing OCCAM data. The ICESat data was downloaded from the National Snow and Ice Data Center, Boulder, USA.

REFERENCES

1. Zwally, H.J., B. Schutz, W. .Abdalati, J. Abshire, C. Bentley, A. Brenner, J. Bufton, J. Dezio, D. Hancock, D. Harding, T. Herring, B. Minster, K. Quinn, S. Palm, J. Spinhirne, and R. Thomas: ICESat's laser measurements of polar ice, atmosphere, ocean, and land. *Journal of Geodynamics* 34, pp. 405-445, 2002.
2. Forsberg, R., and, H. Skourup: Arctic Ocean Gravity, Geoid and Sea-ice Freeboard Heights from ICESat and GRACE. *Geoph. Res. Letters*, vol. 32, L21502, 2005.
3. Laxon , S., N. Peacock, and D. Smith, High interannual variability of sea ice thickness in the Arctic region, *Nature* 425, 947-950, 2003.
4. Tapley, D. B., S. Bettadpur, J. Ries, P. Thomson, M. Watkins (2004): GRACE measurements of mass variability in the earth system. *Science*, 305, issue 5683, 503-505 [doi: 10.1126/science.1099192]
5. Kwok, R., H.J. Zwally, and D. Yi: ICESat observations of Arctic sea ice: A first look. *Geophysical Research Letters*, vol. 31, L16401, 2004.
6. Forsberg, R. and S. Kenyon: *Gravity And Geoid in The Arctic Region – The Northern Polar Gap Now Filled*. 6 pp., Proc. GOCE Workshop, ESRIN, March 2004.
7. Laxon, S., D. McAdoo (1998): *Satellites provide new insights into polar geophysics*. EOS, Transactions AGU, 79 (6), 69-72.
8. Forsberg, R., M. G. Sideris (1993): *Geoid computations by the multi-band spherical FFT approach*. Manuscripta Geodaetica, 18, pp. 82-90.
9. Moritz, H.: Advanced physical geodesy. Wickmann Verlag, Karlsruhe, 1980.